Random Incidence Transmission Loss of a Metamaterial Barrier System

Srinivas VARANASI[1]; J. S. BOLTON[2]; Thomas SIEGMUND[2]

[1] School of Mechanical Engineering, Purdue University

[2] Ray W. Herrick Laboratories, School of Mechanical Engineering, Purdue University

ABSTRACT

It has been shown previously that a panel comprising a cellular array can yield a normal incidence transmission loss in a specified low frequency range that is significantly larger than that of a homogeneous panel having the same mass per unit area. The cellular metamaterial considered consists of a periodic arrangement of unit plates held in a grid-like frame. However, when the incident sound field is diffuse, the relative advantage of the metamaterial barrier is reduced or eliminated. Here it will be shown through a sequence of experimental measurements that the relative advantage of the metamaterial barrier can be restored by creating a hybrid system consisting of a layer applied to the front surface of the material that causes sound to approach the barrier at normal incidence, and a layer on the rear surface of the material that compensates for the transmission loss minimum that normally follows the peak in a metamaterial barrier transmission loss. In the implementation considered here, the front layer consists of a lattice structure, and the rear layer consists of high performance glass fiber. The role of each of these components will be illustrated using measurements of transmission loss of a 1.2 m square panel system.

Keywords: Metamaterial, sound insulation, random incidence

1. INTRODUCTION

Air-borne noise produced by many real life applications such as aircraft (1), home appliances (2) etc., has a significant low frequency component which needs to be controlled. Conventional barrier materials require high mass per unit area for effective noise reduction in this inertia-controlled frequency region (3). Lightweight barrier solutions have been proposed by researchers addressing this challenge using the ideas of acoustic metamaterials since they were first published by Liu et al. (4). Notable solutions include a slab matrix having distributed resonating elements, typically a heavy mass coated with a soft rubber coating (4, 5), membrane-based materials (6, 7) and plate based materials (8). Investigations were performed employing analytical, computational and experimental methods with a majority of the works using computational and analytical methods (9). But, the proposed solutions were mainly examined subjecting them to a normally incident sound field (4, 10, 7, 11, 12, 13). Experiments were performed using a bench-top setup, namely, a standing wave tube apparatus (14) or a modified version of it (15) to observe their sound transmission loss (STL) characteristics. The standing wave tube apparatus may not provide the best representative characteristics that can be expected of the proposed solutions in real life applications because in real life applications, the sound field is seldom uni-directional and more often diffuse (3, 16). It is known from investigations conducted on conventional barrier materials that the STL that can be achieved in a diffuse field is 5 dB lower than the STL predicted in a normally directed sound field (3). Xiao et al. (8) analytically studied the behavior of metamaterial-based thin plates with attached resonators using the methods of plane wave expansion and effective medium and predicted that the benefit in STL of these materials in a diffuse sound field will be lower than in a normally incident sound field.

The objective of this work is to examine the concept of a Hybrid Metamaterial Panel (HMP) at an application-scale subjecting it to a diffused sound field with its primary constituent being a planar cellular metamaterial (17) proposed by the same authors sandwiched between a sound normalizing layer towards the incident side and a sound absorbing mat on the transmission side. A design of the size 1.22×1.22 m

[1] svaranas@purdue.edu

[2] bolton@purdue.edu

[3] siegmund@purdue.edu

is studied and compared with the behavior of a representative limp panel, again obtained from experiment. Their performance is also compared to their predicted behavior from normal sound incidence based numerical models described in (17).

2. MATERIALS

Figure 1 shows a schematic of the HMP studied in this work, and its components: (a) a sound normalizing layer, (b) a cellular panel, and (c) a sound absorbing mat. The system is oriented such that the sound field is incident on the normalizing layer. The sound normalizing layer is a two-dimensional grid with square unit

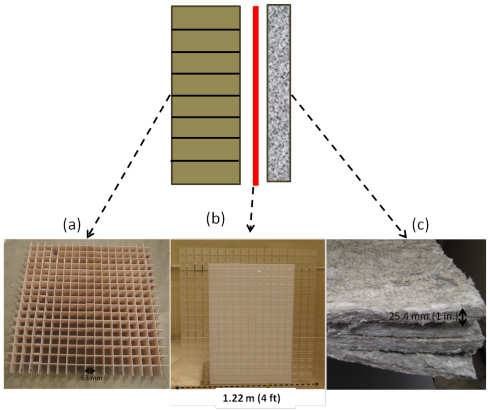

Figure 1 – A schematic of the hybrid metamaterial panel studied in this work with (a) sound normalizing grid (b) cellular panel and (c) sound absorbing mat.

cells of edge length 63.5 mm made from balsa wood strips of thickness 3.175 mm (0.125 in.) and 101.6 mm (4 in.) wide. It acts like a waveguide to make the incident sound field normal by allowing only plane waves to propagate normal to the grid . An ideal rigid-walled grid allows for only those waves which have a propagating component in its normal direction and standing wave modes along the transverse directions (18) for sound frequencies below the cut-off frequency of the lowest non-zero mode: i.e., $c/2L$ where c is the speed of sound in air and L is the longer transverse dimension of the grid unit cell. The chosen edge length of the unit cell of the grid creates a plane wave field for sound waves below 2700 Hz. The overall dimensions of the grid are such that it spans the entire space of the test window exposed to the incident sound field.

The cellular panel was designed using the geometry-based mass apportioning approach of planar cellular metamaterial (17). The outer dimensions of the cellular panel measure 1.22 m (4 ft) $\times$ 1.22 m (4 ft). The area of the panels are spanned by 18 by 18 unit cells and surrounded by a frame of width 4 cm on all four edges. The outer dimensions of the unit cells of the design was taken to be $L_p + 2W_f = 63$ mm (see Fig. 2). The thickness of the unit cell plate (t_p) was chosen to be 1 mm and the in-plane dimension of the unit cell plate (L_p) was chosen to be 51 mm such that the expected high sound transmission loss (STL) region occurs around 1000 Hz. Optically clear cast-acrylic sheet was used to make the design taking into consideration its easy availability and machinability using a CNC Router. The rectangular sheet measures 1.22 m $\times$ 1.22 m with an average measured thicknesses of 12.03 mm. The pockets were milled out of the stock material using a CNC Router. Due to the variation in the thickness of the stock material provided by the vendor and the machining tolerances, the mean thickness of the unit cell plate turned out to be 1.81 mm with an averaged mass per unit area of 5.73 kg/m^2 and a mass contrast, i.e., the ratio of the mass of the frame of the unit cell to the mass of the plate of the unit cell, μ, of 3.5. The elastic modulus of the material was determined to be 3.04 GPa through three-point bend tests which falls within the modulus range specified by the vendor ($2.93 - 3.27$ GPa).

A glass fiber mat (Microlite AA Noise Reduction blankets with a thickness of 25.4 mm (1 inch) and a mass density of 8 kg/m^3) procured from Johns Manville was used as the sound absorbing layer.

The HMP was configured by attaching the sound normalizing layer on the sound incident side and attaching two layers of the mat on the transmitted side using an aluminum tape along the edges of the panel adding an areal mass of 0.45 kg/m^2. The total areal mass of the HMP considered in this work is 6.18 kg/m^2, neglecting the mass of the sound normalizing layer.

An aluminum panel (Al alloy 1100) with a measured average thickness of 2.35 mm (can vary between $2.16 - 2.41$ mm according to the vendor) was used as the representative conventional limp panel. It has an averaged mass per unit area of 6.14 kg/m^2. For a comparative study, a hybrid conventional panel system (HCP) was constructed by replacing the cellular panel with the aluminum panel and retaining the other two components in HMP. The total areal mass of the HCP is 6.59 kg/m^2.

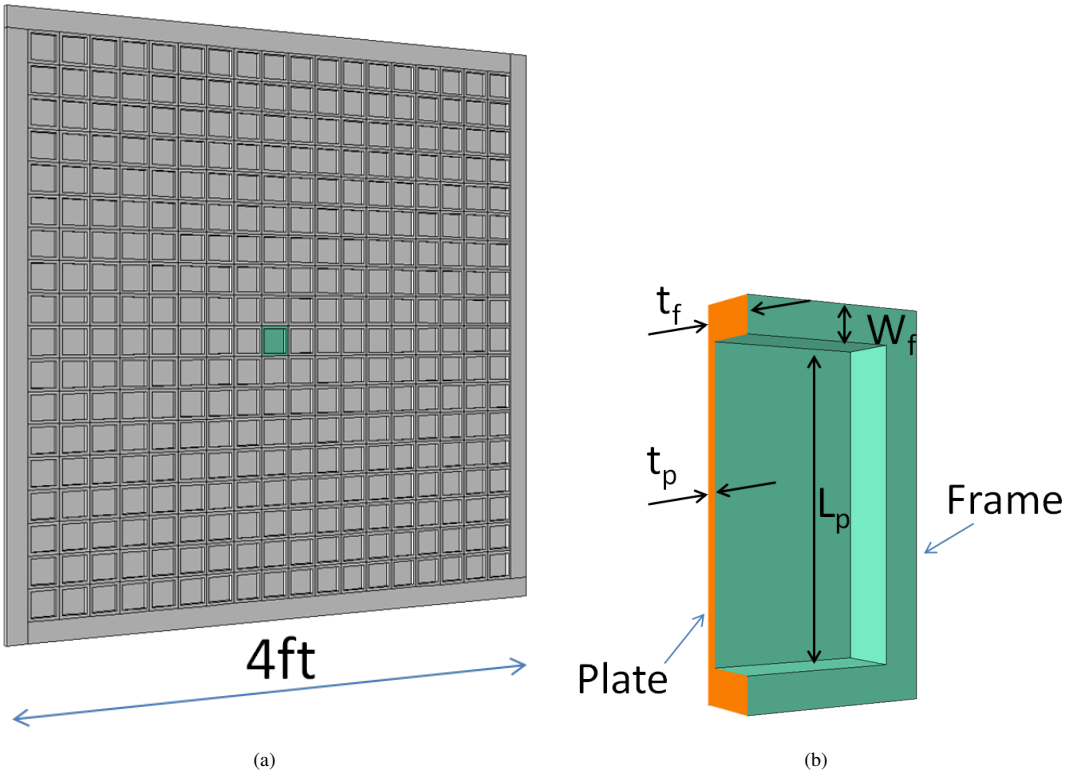

Figure 2 – (a) A schematic of the cellular panel. (b) A cut-section of the unit cell with the dimensions L_p: Edge length of the cell interior, t_p: Thickness of the plate, W_f: Width of the frame and t_f: Thickness of the frame.

3. METHODS

3.1 Experimental setup and measurement procedure

Intensity based methods (19) were used to experimentally study the STL behavior of the specimens subjected to a diffused or randomly incident sound field. The experimental setup (see Fig. 3) primarily consists of a reverberation room and a semi-anechoic termination connected through a window where the test sample is placed. The reverberation room has hard concrete walls with a volume of 254.9 m^3 (9000 ft^3). It has an open window of dimensions 1.22 m (4 ft) by 1.22 m (4 ft) to hold the test specimen. Noise is generated inside the room using two loud speakers (Altec Lansing Model 902 - 8A/B). The speakers were oriented towards the walls away from the window to generate a diffused sound field through multiple reflections by the hard concrete walls. The speakers are driven by two separate random white noise signals generated by B&K Pulse Labshop software interface. The signals have a frequency span of 6.4 kHz with their center frequency being 3.2 kHz, and they were amplified by an SC audio stereo amplifier with Model number 1080. A microphone (B&K pre-polarized free field $1/2$ inch of Type 4189) was stationed in the reverberation room to monitor the sound pressure level inside the room. The test panel was fixed in the window by two wooden frames on either side of the panel which are in turn tightly held in place by clamps from outside. The frame inside the reverberation room is permanently fixed and only the frame on the other side is operated in conducting the experiments. The part of the panel held by the frames is immovable and therefore it is assumed that it does not contribute towards the observed STL. The area of the panel exposed to the incident sound field was hence reduced to 113.4 by 113.4 cm. The panel was sealed all along the edges using an adhesive tape to prevent air leaks from corrupting the intensity probe measurements. The semi-anechoic termination is an assembly of movable walls having thick cones of absorbing material as indicated in the schematic (see Fig. 3) enclosing the window holding the test specimen. A sound intensity probe consisting of a pair of $1/2$ inch B&K Type 4197 microphones separated by a spacer of size 12 mm was used to measure the sound intensity emanating normal to the test panel. The choice of the spacer is the best for a 12.7 mm (1/2 inch) microphone pair to have minimum error in the intensity measurements up to a frequency of 10 kHz (20). A square array of twenty five uniform probe positions were used to sample the intensity of sound at the surface with the aid of a grid constructed using dental floss. The measurements were taken at a distance of 12.7 cm (5 in.) away from the panel on the anechoic termination side as shown in the schematic (see Fig. 3) At the start of each experiment,

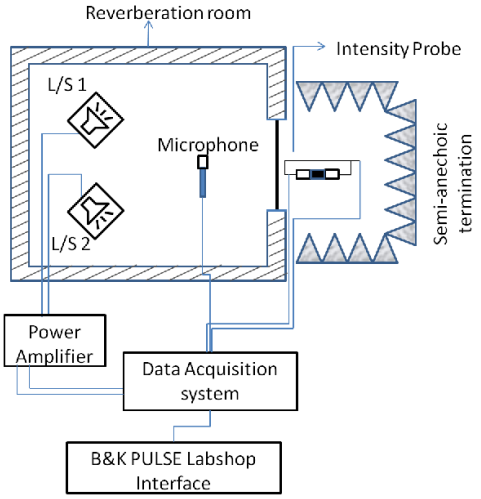

Figure 3 – A schematic of the reverberation room setup for generating a purely diffuse field.

the microphone and the intensity probe were calibrated. The microphone was calibrated using B&K Type 4231 sound source. The intensity probe was calibrated for pressure, velocity and intensity measurements using B&K Type 3541-A calibrator consisting of a piston phone sound source (B&k Type 4228) and a coupler. The pressure-intensity index was checked using a white noise source (B&K Type ZL0055) and the coupler from B&K calibrator Type 3541. The sound pressure level inside the reverberation room was monitored during each experiment and an overall sound pressure level (SPL) of 105 dB was obtained in the reverberation room. Sound intensity was measured at the twenty five probe positions *without* the panel in the window to determine the intensity of sound incident on the test panel. Next, the panel was clamped in the window and the intensity was measured again at the probe positions to determine the sound intensity on the transmitted side. The sound intensity spectrum was measured in $1/12^{th}$ octave bands with the lower and upper center frequencies being 19.31 Hz and 6.131 kHz, respectively. The averaged values of the sound intensity from the twenty five probe points *with* and *without* the panel were used to calculate the averaged STL characteristics of the test panel using the relation

$$STL = -10\log_{10}(\|I_t/I_0\|). \tag{1}$$

Here, I_t and I_0 are the averaged values of the measured intensities from all the probe points *with* and *without* the sound panel in place, respectively.

3.2 Unit cell numerical models

Computer numerical models of the unit cells of the cellular panel design subjected to a normally incident sound field were developed simulating the standing wave tube apparatus (14). These were used to predict the normally incident STL characteristics of the cellular panels similar to the FE models used by the same authors discussed in their work (17). The experimentally determined elastic modulus and the mass density were used in the numerical model.

3.3 Analytical expression for diffused field STL of a limp panel

The analytical expression of diffused sound transmission loss TL_{dif} of a planar limp panel with a mass per unit area of m_s is given by

$$T(\theta) = \frac{2\rho_0 c}{2\rho_0 c + j\omega m_s \cos(\theta)}, \tag{2a}$$

$$\tau(\theta) = \|T(\theta)\|^2 = \frac{4{\rho_0}^2 c^2}{4{\rho_0}^2 c^2 + \omega^2 {m_s}^2 \cos(\theta)^2}, \tag{2b}$$

$$\bar{\tau} = 2\int_0^{90^\circ} \tau(\theta)\sin(\theta)\cos(\theta)\,\mathrm{d}\theta, \tag{2c}$$

$$TL_{dif} = 10\lg_{10}\left(\frac{1}{\bar{\tau}}\right). \tag{2d}$$

Here, θ is the angle of incidence of a sound wave, ρ_0 is the density of air, c is the speed of sound in air, and $\omega = 2\pi f$ where f is the frequency in Hz. $\tau(\theta)$ is the transmission coefficient of a limp panel with an

areal mass m_s for a sound wave incident at an angle θ. The transmission coefficient at normal incidence is given by $\tau(0)$ with the STL for normal incidence TL_{nor} is given by the expression $-10\lg_{10}(\tau(0))$. While the diffused STL (TL_{dif}) defines the lower bound, the normal STL (TL_{nor}) defines the upper bound of the STL characteristics of a limp panel.

4. RESULTS AND DISCUSSION

Figure 4 compares the STL of the cellular panel when subjected to a diffused sound field to that of the numerically predicted STL. The numerical predictions are based on a single unit cell model subjected to a normally incident sound field (described in (17)). Since the cellular panel has a variation in its unit cell thickness t_p, STL predictions for the cases of $(t_p)_{\text{mean}-\sigma}$ and $(t_p)_{\text{mean}+\sigma}$ are plotted. Also, the analytically predicted STL for a mass equivalent limp panel is plotted for reference. It can be seen from this result that (a) the qualitative nature of the experimentally observed STL is consistent with the numerical predictions but the improvement in STL at the peak is reduced, and, (b) the cellular panel performs better in terms of the sTL at its peak region compared to its mass equivalent panel. This result indicates that the nature of the incident sound field has a strong influence on the degree of benefit that can be realized at the peak region of the cellular panels.

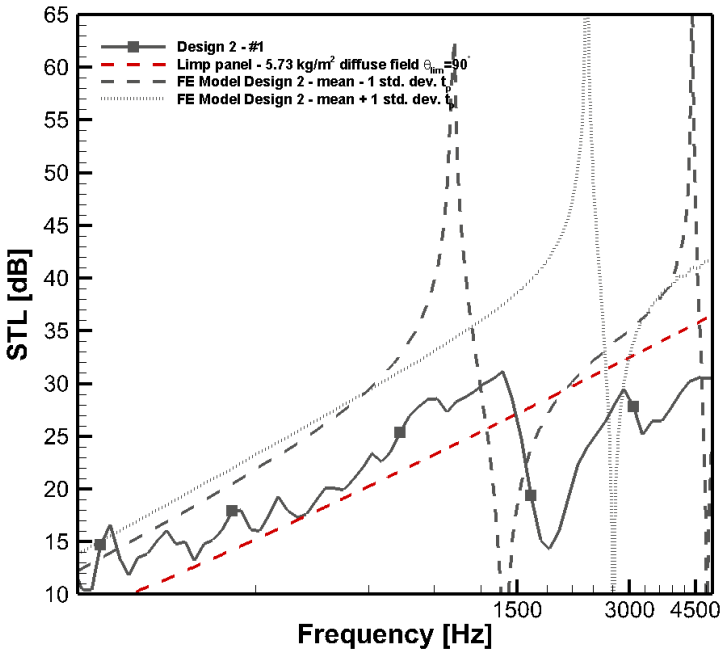

Figure 4 – Comparison of STL characteristics of the cellular panel subjected to a random incident sound field with that of the numerical predicted STL for a normally incident sound field.

Figure 5 shows the experimentally observed STLs of three configurations, namely (a) cellular panel, (b) cellular panel with the sound normalizing layer facing the incident sound field, and (c) with the sound absorbing mat on the transmission side, along with the numerically predicted STLs for the same design. First, it can be observed that the configuration with the sound normalizing layer has significantly improved the benefit in the peak STL region confirming the influence of the nature of the sound field on the observed STL. The improvement is particularly seen at the peak region. Second, the HMP having an absorbing mat on the transmitted side further improved the STL. The improvement in the STL can be seen starting from 600 Hz with the maximum improvement at the peak region. The STL at the dip region which is usually a concern for all the proposed metamaterial solutions to-date has also been remedied through the addition of the sound absorbing mat. This can be seen from Fig. 6 which compares the experimentally observed STL of HMP with that of its mass equivalent limp panel. It can be seen from this plot that the STL of the HMP has a significant improvement over its mass equivalent limp panel, particularly in the peak region. The STL at any frequency including the dip frequency is at least equal to or higher than its mass equivalent limp panel.

Finally, Fig. 7 compares the experimentally observed STLs of the HMP versus the HCP. The HMP has an

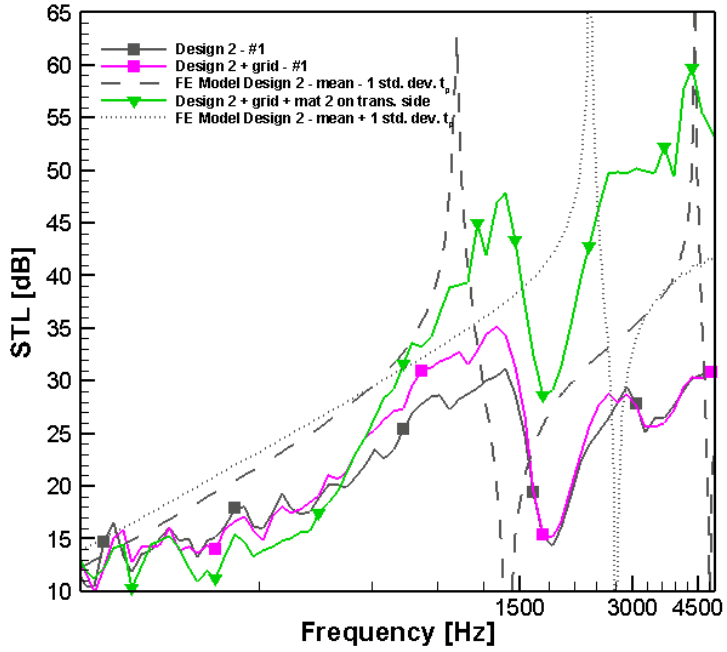

Figure 5 – Comparison of STL characteristics of (a)cellular panel, (b) cellular panel with sound normalizing layer, and (c) cellular panel with sound normalizing layer and absorbing mat (HMP) subjected to a random incident sound field. The numerically predicted STL of the cellular panel for a normally incident sound field is also shown.

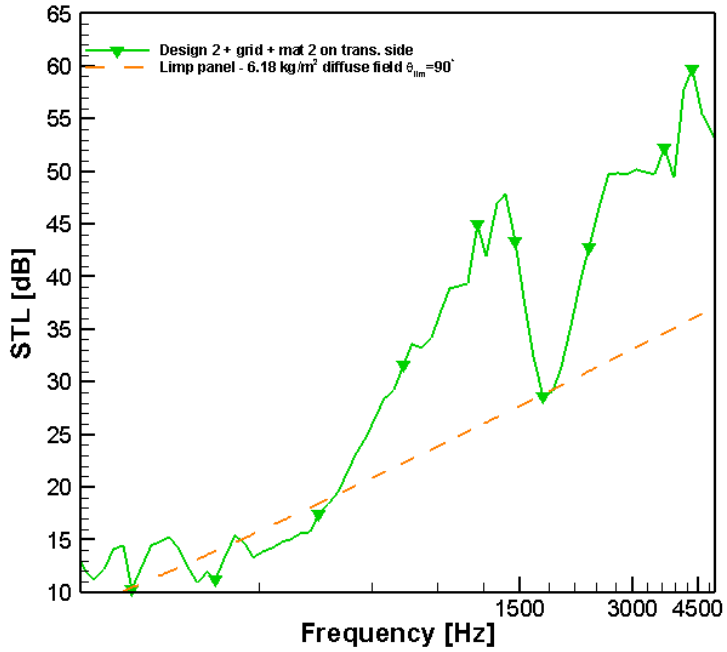

Figure 6 – Comparison of STL characteristics of cellular panel with sound normalizing layer and absorbing mat (HMP) with that of mass equivalent limp panel subjected to a random incident sound field.

areal mass of 6.18 kg/m^2 while the HCP has 6.59 kg/m^2 (6.6% higher than the HMP). From this result, it can be seen that HMP performs better than HCP in a small region around its peak STL. The STL of the HMP is higher

than or at least of the same value as that of HCP for all the frequencies below its peak STL frequency in spite of having 6% lower areal mass than HCP. The relatively modest improvement in transmission loss produced by the metamaterial barrier, in this case, is consistent with its small mass ratio of 3.5. Work previously reported in Ref. (17) indicates that the transmission loss benefit increases as the mass ratio increases, approaching a maximum benefit at a value of approximately 100. Thus it would appear that the current results could be substantially improved upon by altering the metamaterial barrier configuration to increase its mass ratio.

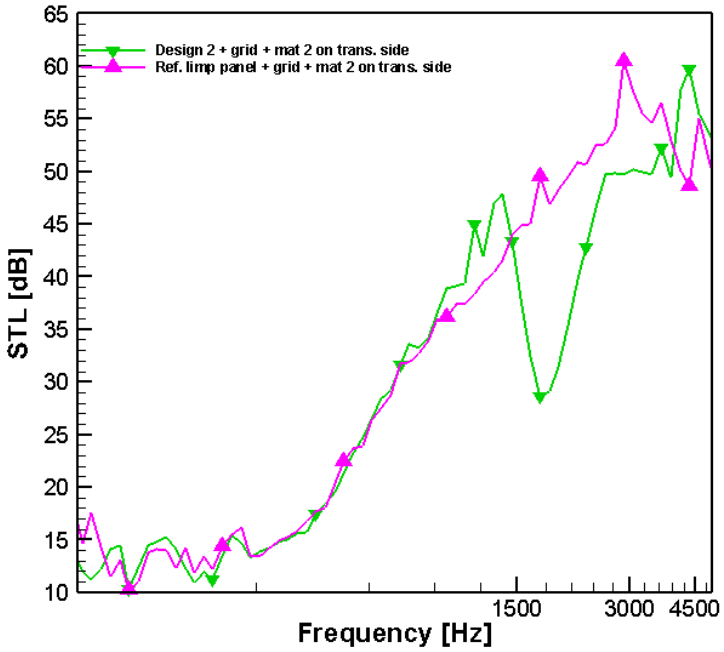

Figure 7 – Comparison of STL characteristics of HMP versus HCP subjected to a random incident sound field.

5. CONCLUSIONS

In this paper, the performance of a metamaterial barrier system under diffuse excitation has been considered. It was found that the diffuse incidence performance of such a barrier is substantially reduced compared to the predicted normal incidence behavior. It was also demonstrated that the performance of the barrier can be improved by the addition of a "normalizing" grid to the front of the panel system, which constrains the incident sound field to approach the panel at normal incidence. Further, the panel performance can be improved by the addition of a sound absorbing mat to the transmission side of the panel system; this mat has the effect of compensating for the reduction in transmission loss in the frequency range immediately above the metamaterial's peak transmission loss. It was further noted that the barrier system demonstrated here showed only a slight improvement with respect to a limp panel of the same mass per unit area in the frequency range of the predicted peak performance, and above that frequency, in fact, the performance of the metamaterial system was worse than that of the corresponding limp panel system. This behavior is consistent with the relatively small mass ratio of the metamaterial barrier considered here (i.e., the ratio of the mass of the cell frame to that of the panel within the cell). Previous numerical work has demonstrated that the benefit of the metamaterial barrier system increases as the mass ratio is increased to at least a value of 100. Thus, in future, it would be desirable to experimentally examine the behavior of metamaterial barrier systems having substantially higher mass ratios.

REFERENCES

1. Wilby JF. Aircraft interior noise. Journal of Sound and Vibration. 1996;190(3):545–564.
2. Jackson GM, Leventhall HG. Household appliance noise. Applied Acoustics. 1975;8(2):101–118.
3. Fahy FJ, Gardonio P. Sound and Structural Vibration: Radiation, Transmission and Response. 2nd ed. Academic Press; 2007.
4. Liu ZY, Zhang XX, Mao YW, Zhu YY, Yang ZY, Chan CT, et al. Locally resonant sonic materials. Science. 2000;289(5485):1734–1736.
5. Wester EC, Brémaud X, Smith B. Meta-material sound insulation. Building Acoustics. 2009;16:21–30.
6. Yang Z, Mei J, Yang M, Chan NH, Sheng P. Membrane-type acoustic metamaterial with negative dynamic mass. Physical Review Letters. 2008;101(20):204301.
7. Naify CJ, Chang CM, McKnight G, Nutt S. Transmission loss and dynamic response of membrane-type locally resonant acoustic metamaterials. Journal of Applied Physics. 2010;108(11):114905.
8. Xiao Y, Wen J, Wen X. Sound transmission loss of metamaterial-based thin plates with multiple subwavelength arrays of attached resonators. Journal of Sound and Vibration. 2012;331:5408–5423.
9. Deymier PA, editor. Acoustic Metamaterials and Phononic Crystals. vol. 173 of Solid-State Sciences. Springer; 2013.
10. Yang Z, Dai HM, Chan NH, Ma GC, Sheng P. Acoustic metamaterial panels for sound attenuation in the 50-1000 Hz regime. Applied Physics Letters. 2010;96(4):041906.
11. Naify CJ, Chang CM, McKnight G, Nutt S. Transmission loss of membrane-type acoustic metamaterials with coaxial ring masses. Journal of Applied Physics. 2011;110(12):124903.
12. Naify CJ, Chang CM, McKnight G, Scheulen F, Nutt S. Membrane-type metamaterials: Transmission loss of multi-celled arrays. Journal of Applied Physics. 2011;109(10):104902.
13. Zhang Y, Wen J, Zhao H, Yu D, Cai L, Wen X. Sound insulation property of membrane-type acoustic metamaterials carrying different masses at adjacent cells. Journal of Applied Physics. 2013;114(6):063515.
14. E2611-09 A. Standard Test Method for Measurement of Normal Incidence Sound Transmission of Acoustical Materials Based on the Transfer Matrix Method. In: ASTM Standards. 100 Barr Harbor Drive, PO Box C700, West Conshohocken, PA 19428-2959, United States: ASTM International; 2009. DOI: 10.1520/E2611-09. Available at `www.astm.org`.
15. Ho KM, Yang Z, Zhang XX, Sheng P. Measurements of sound transmission through panels of locally resonant materials between impedance tubes. Applied Acoustics. 2005;66(7):751–765.
16. Pellicier A, Trompette N. A review of analytical methods, based on the wave approach, to compute partitions transmission loss. Applied Acoustics. 2007;68(10):1192–1212.
17. Varanasi S, Bolton JS, Siegmund TH, Cipra RJ. The low frequency performance of metamaterial barriers based on cellular structures. Applied Acoustics. 2013;74(4):485–495.
18. Kinsler LE, Frey AR, Coppens AB, Sanders JV. Fundamentals of Acoustics. vol. 1. 4th ed. Wiley-VCH; 1999.
19. Bolton JS, Shiau NM, Kang YJ. Sound transmission through multi-panel structures lined with elastic porous materials. Journal of Sound and Vibration. 1996;191(3):317–347.
20. Jacobsen F, Cutanda V, Juhl PM. A numerical and experimental investigation of the performance of sound intensity probes at high frequencies. The Journal of the Acoustical Society of America. 1998;103(2):953–961.